

Energy-level statistics at the metal-insulator transition in anisotropic systems

Frank Milde, Rudolf A. Römer, and Michael Schreiber

Institut für Physik, Technische Universität, D-09107 Chemnitz, Germany

(*Revision* : 3.1; printed June 13, 2019)

Abstract

We study the three-dimensional Anderson model of localization with anisotropic hopping, i.e., weakly coupled chains and weakly coupled planes. In our extensive numerical study we identify and characterize the metal-insulator transition using energy-level statistics. The values of the critical disorder W_c are consistent with results of previous studies, including the transfer-matrix method and multifractal analysis of the wave functions. W_c decreases from its isotropic value with a power law as a function of anisotropy. Using high accuracy data for large system sizes we estimate the critical exponent $\nu = 1.45 \pm 0.2$. This is in agreement with its value in the isotropic case and in other models of the orthogonal universality class. The critical level statistics which is independent of the system size at the transition changes from its isotropic form towards the Poisson statistics with increasing anisotropy.

71.30.+h, 72.15.Rn, 73.20.Dx

I. INTRODUCTION

It is well known that the isotropic Anderson model of localization¹ exhibits a metal-insulator transition (MIT) for spatial dimensions larger than two.²⁻⁴ A critical amount of disorder W_c is necessary to localize all the eigenstates. The asymptotic envelopes of the localized states for $W > W_c$ decay exponentially in space due to the destructive interference of the disorder-backscattered wave functions with themselves. An electron confined in such a state cannot contribute to charge transfer at temperature $T = 0$. For $W < W_c$ there exist states that are extended through the whole sample allowing charge transfer through the system at $T = 0$. In spatial dimensions up to two an arbitrarily small amount of disorder localizes all states and there is no MIT at finite W for non-interacting systems.^{2,3}

In the present study we consider the problem of Anderson localization in three dimensional (3D) disordered systems with anisotropic hopping. One might expect that increasing the hopping anisotropy, namely reducing the hopping probability in one or two directions, is effectively equivalent to changing the dimensionality of the system continuously from 3D to 2D or 1D similarly to the case of (bi)-fractal lattices.⁴ However, this is not the case: The topology of the lattice is not changed as long as the hopping is non-zero and the dimensionality is still three. Only if the coupling is reduced to zero the dimension jumps from 3D to 2D or 1D. Previous studies using the transfer-matrix method (TMM)⁵⁻⁷ and multifractal analysis (MFA)⁸ showed that an MIT exists even for very strong anisotropy. The values of the critical disorder W_c were found to decrease by a power law in the anisotropy, reaching zero only for the limiting 1D or 2D cases. In the present work, we focus our attention on the critical properties of this MIT. As an independent check to previous results, we employ energy level statistics (ELS)⁹⁻¹² together with the finite-size scaling (FSS) approach. ELS has been previously applied with much success at the MIT of the isotropic model and it was shown that a size-independent statistics exists at the MIT.^{10,12,13} This *critical* statistics is intermediate between the two limiting cases of Poisson statistics for the localized states and the statistics of the Gaussian orthogonal ensemble (GOE) which describes the spectrum of extended states.¹⁴ We check whether the critical ELS is influenced by the anisotropy.

A major part of our study is dedicated to the determination of the critical exponent ν of this second-order phase transition. In general it is assumed that ν depends only on general symmetries, described by the universality class, but not on microscopic details of the sample. Thus, anisotropic hopping might shift W_c but should not change ν . In order to verify this assumption it is necessary to determine ν with high accuracy for various anisotropies. This is a computationally demanding task and we emphasize that even in numerical studies of the isotropic Anderson model the correct value of ν is still not entirely clear. Recent highly accurate TMM studies report $\nu = 1.54 \pm 0.08$ ¹⁵ and $\nu = 1.58 \pm 0.06$ ¹⁶, but from ELS $\nu = 1.35 \pm 0.15$ ¹⁷ and $\nu = 1.4 \pm 0.15$ ¹³ was found. Also from TMM $\nu = 1.3 \pm 0.1$ for the isotropic system and $\nu = 1.3 \pm 0.1$ and $\nu = 1.3 \pm 0.3$ for two different data sets for the anisotropic system were determined.⁶ As we will show, an accurate estimation of ν requires the computation of large system sizes before FSS can be reliably employed. Using high precision data and taking into account non-linear corrections to scaling¹⁶ we then find $\nu = 1.45 \pm 0.2$.

The paper is organized as follows. In Sec. II we introduce our notation. We recall the use of ELS for the characterization of the MIT in Sec. III. Using the fact that the statistical

properties at the transition do not depend on the system size, we corroborate the existence of the MIT and determine the anisotropy dependence of the critical disorder and of the critical statistics. In particular, we show that the critical ELS changes continuously with increasing anisotropy from its functional form at the isotropic MIT towards Poisson statistics. In Sec. IV we describe the concept of FSS and the numerical methods to determine the critical properties such as ν . Then we demonstrate that the scaling concept applies to the integrated Δ_3 statistics from ELS¹⁷ and we estimate ν from highly accurate ELS data obtained for very large system sizes. In Sec. V we also check whether our results are compatible with highly accurate TMM data. Finally, we summarize our results in Sec. VI.

II. THE ANISOTROPIC ANDERSON MODEL OF LOCALIZATION

The Anderson model is a standard model for the description of disordered systems with Hamiltonian given as¹

$$H = \sum_i \epsilon_i |i\rangle\langle i| + \sum_{i \neq j} t_{ij} |i\rangle\langle j| \quad . \quad (1)$$

The states $|i\rangle$ are orthonormal and correspond to particles located at sites $i = (x, y, z)$ of a regular cubic lattice with size N^3 . We use periodic boundary conditions $(x + N, y, z) = (x, y + N, z) = (x, y, z + N) = (x, y, z)$. The potential site energies ϵ_i are uniformly distributed in the interval $[-W/2, W/2]$ with W defining the disorder strength, i.e., the amplitude of the fluctuations of the potential energy. The transfer integrals t_{ij} are restricted to nearest neighbors and depend only on the three spatial directions, so t_{ij} can either be t_x , t_y or t_z . We study two possibilities of anisotropic transport: (i) *weakly coupled planes* with

$$t_x = t_y = 1, t_z = 1 - \gamma \quad (2)$$

and (ii) *weakly coupled chains* with

$$t_x = t_y = 1 - \gamma, t_z = 1 \quad . \quad (3)$$

This defines the strength of the hopping anisotropy $\gamma \in [0, 1]$. For $\gamma = 0$ we recover the isotropic case, $\gamma = 1$ corresponds to N independent planes or N^2 independent chains.

III. ENERGY LEVEL STATISTICS

A. ELS and MIT

The statistical properties of the energy spectra reflect the character of the eigenstates and have been proven to be a powerful tool for characterizing the MIT.^{9–13,17} On the insulating side of the MIT, one finds that localized states that are close in energy are usually well separated in space whereas states that are localized in vicinal regions in space have well separated eigenvalues. Consequently, the eigenvalues on the insulating side are uncorrelated, there is no level repulsion and the probability of eigenvalues to be close together is high. This is called level clustering and is described by the Poisson statistics.¹⁴ On the

other hand, extended states occupy the same regions in space and their eigenvalues become correlated. This results in level repulsion such that the spectral properties are given by the GOE statistics.¹⁴

In an infinitely large disordered system, the MIT corresponds to a sharp transition from GOE statistics at the metallic side to Poisson statistics at the insulating side via some intermediate critical statistics only exactly at the critical point.^{10,12} In a finite system, this abrupt change is smeared out, because the divergence of the characteristic lengths — such as the localization length — of the wave functions at the phase transition is cut off at the system size. If for a given W the localization length in the infinite system is much larger than the system size under consideration, the states appear to be extended in the finite system. Their eigenvalues become correlated and the ELS is changed from Poisson towards GOE statistics. To obtain a reliable characterization of the MIT one should therefore investigate the system-size dependence of the spectral properties: With increasing system size there is a trend towards the limiting cases of GOE and Poisson statistics for the extended and localized regions, respectively. Directly at the critical disorder there are no characteristic length scales, the wave functions are scale-invariant multifractal entities^{8,18} and the statistical properties of the spectrum are independent of the system size.^{10,12}

B. The numerical approach

In ELS a system is characterized by the local fluctuations of the energy spectrum around its average density of states (DOS) $\bar{\rho}(E)$.¹⁴ Usually, $\bar{\rho}(E)$ is not constant for a given sample and has different width or even different shape for different samples. We therefore apply a so-called unfolding procedure¹¹ to map the set of eigenvalues $\{E_i\}$ to a new set $\{\varepsilon_i\}$ with constant average density equal to unity as required for the application of random matrix theory.¹⁴ We then characterize the unfolded spectrum $\{\varepsilon_i\}$ by the distribution $P(s)$, which measures the level repulsion in terms of the nearest-neighbor level-spacing s , by the cumulative level-spacing distribution $I(s) = \int_s^\infty P(s')ds'$, and by the Δ_3 statistics, which measures the deviation from a sequence of L uniformly spaced levels,^{11,14}

$$\Delta_3(L) = \left\langle \frac{1}{L} \min_{A,B} \int_\varepsilon^{\varepsilon+L} [D(\varepsilon') - A\varepsilon' - B]^2 d\varepsilon' \right\rangle_\varepsilon . \quad (4)$$

Here, $D(\varepsilon)$ is the integrated DOS and $\langle \rangle_\varepsilon$ corresponds to averaging over the spectrum.

For the eigenvalue computation the Lanczos algorithm in the Cullum-Willoughby implementation^{19,20} is applied which is very effective for our sparse matrices.²¹ We use system sizes up to $N = 50$ for which a 400 MHz Pentium II machine needs about five days for the diagonalization of a single system. The character of the eigenstates has been shown not to change in a large energy interval around $E = 0$.²² For the computation of the spectral properties we therefore use an interval centered at $E = 0$ containing 50% of the eigenvalues.^{11,13} Furthermore we average over a number of configurations of the potential site energies such that at least 10^5 , but typically 2×10^5 to 4×10^5 , eigenvalues contribute to $P(s)$, $I(s)$ or $\Delta_3(L)$ for every N , W , and γ . Altogether we investigated about 750 such parameter combinations.

C. Dependence of W_c on anisotropy

As expected, we find a crossover from GOE statistics to Poisson statistics with increasing W for all values of γ considered and both, coupled planes and chains. As an example we show $I(s)$ for weakly coupled chains in Fig. 1. This crossover is a first hint for the existence of an MIT. In order to check this further we investigate the system-size dependence of the Δ_3 statistics. In Fig. 2 we show $\Delta_3(L)$ for weakly coupled planes for various system sizes. There is a clear trend towards GOE and Poisson statistics for $W = 6$ and $W = 12$, respectively. But there is hardly any system-size dependence visible for $W = 8.625$. As described above, this indicates an MIT with a critical disorder in the vicinity of $W = 8.625$. For a more accurate determination of W_c , we consider the integral $\alpha_N(W) = \int_0^{30} \Delta_3(L, W, N) dL$ as a function of W for several system sizes N .¹² As can be seen from Fig. 2, the value of α_N monotonically increases as the ELS changes from GOE to Poisson statistics. In the localized region α_N will therefore increase with N , whereas it will decrease with N for extended states. One can then determine W_c from plots of $\alpha_N(W)$ for different N as shown, e.g., in Fig. 3 for $\gamma = 0.9$. All curves cross in one point, at which the size effects change sign. This indicates the transition which occurs at $W_c = 8.6 \pm 0.2$ in this case. Our results for other values of γ are compiled in Fig. 4. We find that with increasing anisotropy the critical disorder decreases according to a power law $W_c = 16.5(1 - \gamma)^\beta$ with $\beta \approx 0.25$ for coupled planes and $\beta \approx 0.6$ for coupled chains. As shown in Fig. 4 this is an appropriate description for our ELS data and agrees well with the results of our previous MFA.⁸ For coupled planes this result is also consistent with a previous TMM study and a perturbative analysis employing the coherent potential approximation (CPA)⁶ but in the case of coupled chains $\beta \approx 0.6$ appears more appropriate than the result $\beta = 0.5$ of Ref. 6.

D. Dependence of $P_c(s)$ on anisotropy

Let us now turn our attention to the question whether the form of the size-independent statistics at the MIT $P_c(s)$ depends on anisotropy. It seems to be settled — at least for the isotropic case — that the small- s behavior of $P_c(s)$ is equal to that of the metallic phase with $P_c(s) \propto s$ as usual for the orthogonal ensemble, s^2 for the unitary, and s^4 for the symplectic ensembles.^{23,24} Furthermore, it was shown that the large- s behavior of $P_c(s)$ and $I_c(s)$ can be described by an exponential decay $P_c(s) \propto I_c(s) \propto e^{-A_c s}$ with $A_c \approx 1.9$ for all three universality classes.^{13,17,23,24} All these studies were performed for 3D using periodic boundary conditions and cubic samples. On the other hand, $P_c(s)$ has been shown to depend on the sample shape²⁵ and on the applied boundary conditions as well.^{26,27} A trend towards Poisson behavior was found when the cube was deformed by increasing or decreasing the length in one direction²⁵ or when periodic boundary conditions were changed to Dirichlet in one, two, or three directions.^{26,27} Thus A_c decreases from 1.9 towards 1. Furthermore, A_c depends on the dimensionality since in the orthogonal 4D case the critical $P_c(s)$ was found to be closer to Poisson statistics than in 3D.²⁸ From the 4D results one might expect the opposite effect for our coupled planes and chains. This is not the case and we also find a trend towards Poisson statistics for increasing γ as can be seen, e.g., in Fig. 5 for coupled planes. This finding is consistent with the MFA results⁸ where the singularity spectra at the transition were found to tend towards the localized behavior with increasing anisotropy.

While investigating the dependence on the sample shape we observe another interesting behavior. In the isotropic case, when deforming the cubic sample to a cuboid, the statistical properties of the spectra always tend towards Poisson statistics, irrespective of whether the sample becomes a long quasi-1D bar or a flat quasi-2D sample.²⁵ Here we compute $I(s)$ for coupled planes with $\gamma = 0.9$ at $W = W_c = 8.625$ for two cases: (i) bar-shaped samples of size $10 \times 10 \times 100$ extending in the direction with reduced hopping and (ii) flat samples of size $50 \times 50 \times 5$ with large weakly coupled planes. We insert the results into Fig. 5. Surprisingly we find an opposite trend for the two cases: (i) for the bars $I(s)$ is close to Poisson statistics, very similar to $I_c(s)$ for $\gamma = 0.99$; (ii) for the flat samples $I(s)$ is close to GOE statistics and the isotropic $I_c(s)$ is nearly recovered. This result is probably due to the fact, that the system sizes in case (ii) are proportional to the localization lengths, which depend on the direction.⁶ The extension of the wave function measured in units of its characteristic lengths is then equal in all directions. We remark that a similar observation in 2D anisotropic samples exists: the isotropic scaling function is recovered, if the dimensions of the system are proportional to the localization lengths.²⁹ We expect that a further increase of the aspect ratio, i.e., reduction of the system towards 2D, will drive $I(s)$ again towards Poisson statistics. But this needs further study.

We remark, that the increasing fluctuations for $s > 6$ in the $I(s)$ curves in Fig. 5 are due to the fact, that there are only very few such large spacings. Consequently, there is no good statistics. In tests with large Poisson sequences of up to 10^6 eigenvalues, we find similar small but increasing deviations from the theoretical result for $s > 6$.

IV. ONE-PARAMETER SCALING AT THE MIT

The MIT in the Anderson model of localization is expected to be a second-order phase transition,^{2,30} which is characterized by a divergence in an appropriate correlation length

$$\xi_\infty(W) = C|W - W_c|^{-\nu} \quad (5)$$

with critical exponent ν , where C is a constant.³ Here $\xi_\infty(W)$ is the correlation length of the *infinite* system, but in practice only finite, and still relatively small, systems are numerically accessibly. In order to construct a thermodynamic limit, scaling laws $X(W, bN) = F(X(W, N), b)$ are applied to the finite-size data $X(W, N)$. Here X denotes a dimensionless system property to be specified later and b is an arbitrary scale factor.³¹ The scaling law has solutions of the form

$$X = f(N/\xi_\infty) \quad (6)$$

which implies that the system size N can be scaled by $\xi_\infty(W)$ such that all $X(W, N)$ collapse onto a single scaling function f . For a system with an MIT, this scaling function consists of two branches corresponding to the localized and the extended phase. In numerical experiments the reduced localization length $\Lambda_N(W)$ obtained by the TMM is often used as quantity X .^{3,6,32,33} Scaling has also been shown for quantities derived from ELS, particularly for $\alpha_N(W)$ defined in Sec. III C.^{10,12}

For the estimation of the critical exponent ν , one can numerically perform the FSS procedure³⁴ in order to determine the scaling function $f(N/\xi_\infty)$ by minimizing the deviations

of the data from the common scaling curve. After construction of the scaling curve, one can then fit the obtained scaling parameters $\xi_\infty(W)$ according to Eq. (5). However, the divergence of $\xi_\infty(W)$ at W_c is rounded because of numerical inaccuracies.³⁴ On the other hand, Eq. (5) is not expected to be valid far away from W_c and it is a priori very difficult to determine an appropriate disorder range for the fit.

There are several possibilities of determining ν directly from $X(W, N)$, thereby avoiding the numerical inaccuracies introduced by the scaling procedure. Linearizing Eq. (6) at the transition and using Eq. (5) one finds that close to W_c the quantity X behaves as³

$$X(W, N) = X(W_c, N) + \tilde{C}(W - W_c)N^{1/\nu} \quad . \quad (7)$$

Fitting the linear range of $X(W)$ for various fixed values of N now allows us to determine ν . One can also find a similar expression where X is replaced by $\ln X$.¹⁵ Although both expressions are equivalent close to the MIT, they can give different results due to finite precision numerics. Another complication appears due to the presence of a systematic shift of the crossing point of the $X(W)$ curves visible, e.g., in highly accurate TMM data.^{15,16} Such a shift occurs also in our ELS data, but it is less prominent than in the mentioned TMM studies and can barely be seen in the inset of Fig. 3. The shift is not described by Eq. (7). The first attempt to overcome this problem was adding a correction term B to Eq. (7) which depends on N but not on W .¹⁵ This correction allows us to determine ν without an assumption about the nature of the shift. However, the value of W_c is not accessible in this procedure since a change in W_c can be compensated by changing the correction $B(N)$ accordingly.

Alternatively one can assume that the small deviations from one-parameter scaling are caused by an irrelevant scaling variable, i.e., the presence of additional terms in (7) with system-size dependence N^y , with $y < 0$, which vanish for large system sizes. This approach takes into account that the shift is not random but rather appears to be systematic. We use such a method introduced recently.¹⁶ A family of fit functions is constructed, which includes two kinds of corrections to scaling: (i) an irrelevant scaling variable and (ii) nonlinearities of the disorder dependence of the scaling variables. Starting point is the renormalization group equation (or scaling function) for X

$$X = \tilde{f}(\chi_r N^{1/\nu}, \chi_i N^y) \quad . \quad (8)$$

χ_r and χ_i are the relevant and irrelevant scaling variables with corresponding critical and irrelevant exponents ν and y , respectively. \tilde{f} is then Taylor expanded up to order n_i in terms of the second argument

$$X = \sum_{n=0}^{n_i} \chi_i^n N^{ny} \tilde{f}_n(\chi_r N^{1/\nu}) \quad , \quad (9)$$

and each \tilde{f}_n is Taylor expanded up to order n_r :

$$\tilde{f}_n = \sum_{i=0}^{n_r} a_{ni} \chi_r^i N^{i/\nu} \quad . \quad (10)$$

Finally, nonlinearities are taken into account by expanding χ_r and χ_i in terms of $w = (W_c - W)/W_c$ up to order m_r and m_i , respectively,

$$\chi_r(w) = \sum_{n=1}^{m_r} b_n w^n, \quad \chi_i(w) = \sum_{n=0}^{m_i} c_n w^n \quad , \quad (11)$$

with $b_1 = c_0 = 1$. Choosing the orders n_i, n_r, m_r, m_i up to which the expansions are carried out, one can adjust the fit function to the data set. If there is a single crossing point, an irrelevant scaling variable is not necessary and n_i is set to zero. In order to recover the linear behavior (7), one chooses $n_r = m_r = 1$ and $n_i = m_i = 0$. However, we emphasize that the linear region around W_c is very small and a simple scaling with Eq. (7) will not give accurate results. For larger W ranges, 2nd or 3rd order terms are necessary for the fit. Setting n_r or m_r to two or three yields appropriate fit functions. The total number of fit parameters including W_c, ν , and y is $N_p = (n_i + 1)(n_r + 1) + m_r + m_i + 2$ and should of course be kept as small as possible.

There is a alternative method developed for ELS which should give very accurate results with a relatively small number of data points.¹⁷ The data $X(W)$ for constant N are fitted with third-order polynomials and these functions are used to generate a large number of new data points for which the FSS procedure³⁴ is employed. This saves a lot of computer time but does not solve the problems of the FSS procedure discussed above. Furthermore, this smoothing pretends a higher quality of the data than actually achieved.

V. COMPUTATION OF THE CRITICAL PROPERTIES AT THE MIT

We have decided to determine the critical exponent ν for coupled planes with strong anisotropy $\gamma = 0.9$ with highest accuracy. We therefore doubled the number of samples for this value of γ compared to the other cases and used large system sizes, namely $N = 13, 17, 21, 24, 30, 40$, and 50. The disorder range is $W \in [6, 12]$ except for $N = 50$ where we reduced it to $W \in [8, 9.25]$. These data are shown in Fig. 3. Here, 5×10^5 to 7×10^5 eigenvalues contribute to each $\alpha_N(W)$ and the statistical error from the average over the α_N values from each sample is between 0.2% and 0.4%. The number of samples ranges from 699 for $N = 13$ to 10 for $N = 50$.

A. The non-linear fit

For the non-linear fit to the data, we use the Levenberg-Marquardt method³⁵ (LMM) as implemented, e.g., in the *Mathematica* function `NonlinearRegress`. The LMM minimizes the χ^2 statistics, measuring the deviation between model and data under consideration of the error of the data points. In order to judge the quality of the fit, we use the goodness-of-fit parameter Q ,³⁵ which incorporates besides the value of χ^2 also the number of data points and fit parameters. For reliable fits Q should fall into the range $0.01 < Q < 1$.³⁵ The output of the LMM routine contains also confidence intervals for the estimated fit parameters. We check these independently by computing a number of new data sets by randomly varying each data point $\alpha_N(W)$ within its error bar. The LMM fit procedure is then applied to these new sets and the variance of the resulting W_c and ν values is compared to the confidence intervals of the original fit. We find that they do not differ significantly. More importantly, we also check whether the fit parameters are compatible when using different expansions of

the fit function as outlined in the last section. As we will show below, it turns out that then the fitted values of W_c and ν differ from each other by more than the confidence intervals obtained from the individual LMM fits. This is important when coalescing all of them into a final result.

B. Results

In the ELS data we do not find a clear shift of the crossing point up to the accuracy of our data as shown in Fig. 3. Therefore, an irrelevant scaling variable is probably not necessary when using the FSS of Sec. IV and we usually set $n_i = 0$. However, the nonlinearities in the W dependence of α_N require fit functions with W^3 terms, i.e., $n_r \geq 3$ or $m_r \geq 3$. E.g., our choice $n_r = 3$, $m_r = 1$ yields the fit function

$$\alpha_N = a_{00} + a_{01}N^{1/v}w + a_{02}N^{2/v}w^2 + a_{03}N^{3/v}w^3 \quad . \quad (12)$$

To achieve a good quality of fit while avoiding higher orders of the expansions than 3, we use the reduced W interval [7, 11] in the fits. Additionally, the interval $W \in [8, 9.25]$ where we have data for $N = 50$ is employed and we vary the N interval in order to find a possible trend when using larger system sizes only. In Table I the parameters of the fit function, χ^2 , Q and the results for W_c and ν with their confidence intervals are summarized. We report the best fits obtained for five combinations of N and W intervals as denoted by the characters A to E. For completeness, a few worse fits, denoted by small characters, are added. First one notices that the quality of fit is rather good for most cases, i.e., $Q > 0.8$. Only for group B, we find smaller values $Q = 0.13 - 0.22$ which nevertheless still indicate a useful fit. Thus the fit functions describe the data very well. This can be also seen in Fig. 3, where we added the fitted model functions of fit A. As shown in Fig. 6, the data collapse onto a single scaling function with two branches corresponding to the localized and extended regime. This indicates, together with the divergent scaling parameter shown in the inset of Fig. 6, clearly the MIT. The values of the critical disorder obtained from the different fits are scattered from 8.54 to 8.62 although the 95% confidence intervals as given by the LMM are ± 0.02 only. Apparently, these error estimates do not characterize the real situation. Thus, we conclude $W_c = 8.58 \pm 0.06$. For the critical exponent the situation is even worse as visualized in Fig. 7. The results scatter from 1.26 up to 1.51. Some of the 95% confidence intervals which range from ± 0.04 to ± 0.10 overlap but others are far apart. Consider for instance group C: while both fits have a Q value of nearly one, their estimates for ν differ by twice the width of the confidence intervals. This is unexpected since the standard deviation of the α_N values is taken into account by the LMM. We have also tested the use of an energy interval containing only 20% of the eigenvalues instead of 50% for the determination of the α_N data, because one might argue that the ELS and thus the critical behavior depends on E more strongly in the anisotropic case than in the isotropic system where no changes were found for a large E interval.²² However, we find no significant changes of the results in the anisotropic case, either.

An interesting trend can be seen by considering the mean value of the fitted ν within the groups. For A and B it is 1.28 and 1.32, for the three other groups C,D,E, where the data for smaller system sizes ($N = 13, 17, 21$) are neglected, the mean ν is 1.42, 1.45, and 1.42.

The fitted critical exponent apparently increases if only larger system sizes are considered. This is a hint that in the thermodynamic limit ν is probably larger than 1.4. And it also might indicate that there are finite-size corrections in the α_N data that are not described by the fit functions. Considering this trend and the scattering of the results from all fits we conclude from our ELS data the critical exponent $\nu = 1.45 \pm 0.2$. This is consistent with other ELS results for the orthogonal case, $\nu = 1.34 \pm 0.10$ ¹² and 1.4 ± 0.15 ¹³. As our results are obtained from more accurate data due to more samples and larger system sizes, and in the light of the above discussion, we believe that the error estimates of Refs. 12,13 are too small. Our ν is small compared to results from highly accurate TMM studies. For the present case of weakly coupled planes $\nu = 1.62 \pm 0.08$ was obtained.³⁶ For the isotropic case without magnetic field $\nu = 1.54 \pm 0.08$ ¹⁵ and $\nu = 1.58 \pm 0.06$ ¹⁶ was determined. However, considering the error bars obtained from the scattering of the results from different fits, the results are consistent.

As a further test to check whether the results from TMM and ELS are compatible, we scaled the $\alpha_N(W)$ data with the scaling parameter $\xi_\infty(W)$ available from FSS of TMM data with 0.07% accuracy.³⁶ As can be seen in Fig. 8, the α_N data collapse reasonably well onto a single scaling function. Apparently, the $N = 50$ data lie systematically slightly above the scaling function. We remark that in our calculations, the seed that initializes the random number generator depends only on the number of the sample but not on the value of W . The potential energies for the k th sample are obtained by scaling the k th sequence of random numbers with W . For a small number of samples, i.e., 10 for $N = 50$, this might lead to the observed systematic shift. Another possible reason is, that the influence of an irrelevant scaling variable starts to become visible. But using such a variable in the fits gives no improvement of the results although the number of parameters increases remarkably. In group g of Table I we report a few of such fits. Compared to group B the Q values are much larger. But for the first two fits the confidence intervals are extremely large and the estimates for ν and W_c are nearly meaningless. The third fit gives essentially the same results as the corresponding fit of group B. We remark that one has to be very careful when using such non-linear fits. Even an excellent Q value does not guarantee useful results for the fitted model parameters.

For completeness we also used the fit method¹⁷ described at the end of Sec. IV. The third-order polynomials are shown in the inset of Fig. 3 and the scaled data in Fig. 6. The scaling is almost perfect, which is not surprising because of the effective smoothing of the data by means of the cubic fits. The scaling function is very similar to that from fit f which gives the same critical exponent $\nu \approx 1.3$. But as mentioned before, it is very difficult to derive a reliable ν and its error estimate with this method.

VI. SUMMARY

In the present work we have studied the metal-insulator transition in the 3D Anderson model of localization with anisotropic hopping. We used ELS together with FSS analysis to characterize the MIT. Our results indicate in agreement with previous studies that a transition exists for any anisotropy $\gamma < 1$ for coupled planes and for coupled chains. We find a power-law decay of the critical disorder with increasing anisotropy. For coupled chains the decay is found to be faster than predicted by previous CPA results.⁶ A large part of

the present work is devoted to the determination of the critical exponent ν . We calculated the integral $\alpha_N(W)$ over the Δ_3 statistics with very large system sizes and high accuracy for the case of coupled planes with $\gamma = 0.9$. In order to determine ν we used a method to fit the data introduced by Slevin and Ohtsuki¹⁶ which allows for corrections to scaling due to an irrelevant scaling variable and nonlinearities in the disorder dependence of the scaling variables. It turns out that it is not necessary to take into account an irrelevant scaling variable. By varying the ranges of system size and disorder we find a large number of fits, which all describe the data remarkably good. One expects that the estimates for ν from all these fits are consistent within the error bars. Unfortunately, the 95% confidence intervals do not always overlap. Apparently, the error estimate from the fit procedure does not reflect the possible fluctuations in ν . Furthermore, we find a systematic shift towards larger values of ν if only the largest system sizes are considered. This might indicate the existence of finite-size corrections not included in the ansatz. Taken all these into account we conclude $\nu = 1.45 \pm 0.2$. Considering the accuracy of our data and the large system sizes used, this error estimate appears surprisingly large when compared to previous estimates. We presume that most specified errors in similar studies are somewhat optimistic. Within the error bars, our result is consistent with highly accurate TMM studies for the GOE case.^{36,16,15} This supports the concept of universality classes, from which one expects no change of the critical exponent for anisotropic hopping.

The ELS data at the MIT are independent of the system size, but they depend on anisotropy. For increasing anisotropy we find a trend from the isotropic form towards Poisson statistics. Since it was found that the critical statistics also depends on boundary conditions and on the shape of the sample,²⁵⁻²⁷ as well as on the dimensionality,²⁸ one might doubt the validity of the very attractive concept of a super universality class¹⁷ characterizing the critical point in all universality classes. That concept is based on the observation of very similar critical exponents and agreement of the large- s behavior of $P(s)$ at W_c in the isotropic Anderson model. We believe that at present the accuracy in the determination of the critical properties does not allow for an entirely convincing validation of this concept.

ACKNOWLEDGMENTS

This work was supported by the DFG within the Sonderforschungsbereich 393.

REFERENCES

- ¹ P. W. Anderson, Phys. Rev. **109**, 1492 (1958).
- ² E. Abrahams, P. W. Anderson, D. C. Licciardello, and T. V. Ramakrishnan, Phys. Rev. Lett. **42**, 673 (1979).
- ³ B. Kramer and A. MacKinnon, Rep. Prog. Phys. **56**, 1469 (1993).
- ⁴ M. Schreiber and H. Grussbach, Phys. Rev. Lett. **76**, 1687 (1996).
- ⁵ Q. Li, C. Soukoulis, E. N. Economou, and G. Grest, Phys. Rev. B **40**, 2825 (1989).
- ⁶ I. Zambetaki, Q. Li, E. N. Economou, and C. M. Soukoulis, Phys. Rev. Lett. **76**, 3614 (1996), cond-mat/9704107.
- ⁷ N. Panagiotides and S. Evangelou, Phys. Rev. B **49**, 14122 (1994).
- ⁸ F. Milde, R. A. Römer, and M. Schreiber, Phys. Rev. B **55**, 9463 (1997).
- ⁹ S. Evangelou and E. Economou, Phys. Rev. Lett. **68**, 361 (1992).
- ¹⁰ B. I. Shklovskii, B. Shapiro, B. R. Sears, P. Lambrianides and H. B. Shore, Phys. Rev. B **47**, 11487 (1993).
- ¹¹ E. Hofstetter and M. Schreiber, Phys. Rev. B **48**, 16979 (1993).
- ¹² E. Hofstetter and M. Schreiber, Phys. Rev. B **49**, 14726 (1994), cond-mat/9402093.
- ¹³ I. K. Zharekeshev and B. Kramer, Phys. Rev. Lett. **79**, 717 (1997), cond-mat/9706255.
- ¹⁴ M. L. Mehta, *Random Matrices* (Academic Press, Boston, 1990).
- ¹⁵ A. MacKinnon, J. Phys.: Condens. Matter **6**, 2511 (1994).
- ¹⁶ K. Slevin and T. Ohtsuki, Phys. Rev. Lett. **82**, 382 (1999), cond-mat/9812065.
- ¹⁷ E. Hofstetter, Phys. Rev. B **57**, 12763 (1998), cond-mat/9611060.
- ¹⁸ M. Schreiber and H. Grussbach, Phys. Rev. Lett. **67**, 607 (1991).
- ¹⁹ J. Cullum and R. A. Willoughby, *Lanczos Algorithms for Large Symmetric Eigenvalue Computations, Volume 1: Theory* (Birkhäuser, Boston, 1985).
- ²⁰ J. Cullum and R. A. Willoughby, *Lanczos Algorithms for Large Symmetric Eigenvalue Computations, Volume 2: Programs* (Birkhäuser, Boston, 1985), <http://www.netlib.org/lanczos/>.
- ²¹ U. Elsner, V. Mehrmann, F. Milde, R. A. Römer and M. Schreiber, SIAM J. Sci. Comp. **20**, 2089 (1999), physics/9802009.
- ²² B. Bulka, M. Schreiber, and B. Kramer, Z. Phys. B **66**, 21 (1987).
- ²³ E. Hofstetter, Phys. Rev. B **54**, 4552 (1996), cond-mat/9604100.
- ²⁴ M. Batsch, L. Schweitzer, I. K. Zharekeshev, and B. Kramer, Phys. Rev. Lett. **77**, 1552 (1996), cond-mat/9607070.
- ²⁵ H. Potempa and L. Schweitzer, J. Phys.: Condens. Matter **10**, L431 (1998), cond-mat/9804312.
- ²⁶ D. Braun, G. Montambaux, and M. Pascaud, Phys. Rev. Lett. **81**, 1062 (1998), cond-mat/9712256.
- ²⁷ L. Schweitzer and H. Potempa, J. Phys.: Condens. Matter **10**, L431 (1998), cond-mat/9809248.
- ²⁸ I. Zharekeshev and B. Kramer, Ann. Phys. (Leipzig) **7**, 442 (1998), cond-mat/9810286.
- ²⁹ Q. Li, S. Katsoprinakis, E. N. Economou, and C. M. Soukoulis, Phys. Rev. B **56**, R4297 (1997), cond-mat/9704104.
- ³⁰ D. Belitz and T. R. Kirkpatrick, Rev. Mod. Phys. **66**, 261 (1994).
- ³¹ D. J. Thouless, Phys. Rep. **13**, 93 (1974).
- ³² J.-L. Pichard and G. Sarma, J. Phys. C: Solid State Phys. **14**, L127 (1981).

- ³³ A. MacKinnon and B. Kramer, *Phys. Rev. Lett.* **47**, 1546 (1981).
- ³⁴ A. MacKinnon and B. Kramer, *Z. Phys. B* **53**, 1 (1983).
- ³⁵ W. H. Press, B. P. Flannery, S. A. Teukolsky, and W. T. Vetterling, *Numerical Recipes in FORTRAN*, 2nd ed. (Cambridge University Press, Cambridge, 1992).
- ³⁶ F. Milde, R. A. Römer, and M. Schreiber, to be published (1999).

TABLES

	N	W	n_r	m_r	n_i	χ^2	Q	W_c	ν
A	13...40	7...11	3	1	0	52.6	0.96	8.62 ± 0.02	1.28 ± 0.03
a	13...40	7...11	1	3	0	96.6	0.03	8.60 ± 0.02	1.41 ± 0.03
b	13...50	8...9.25	3	1	0	71.4	0.095	8.59 ± 0.02	1.33 ± 0.08
b	13...50	8...9.25	1	3	0	78.8	0.03	8.58 ± 0.02	1.38 ± 0.06
B	13...50	8...9.25	3	2	0	67.7	0.14	8.59 ± 0.02	1.33 ± 0.08
B	13...50	8...9.25	2	3	0	68.2	0.13	8.60 ± 0.02	1.35 ± 0.06
B	13...50	8...9.25	3	3	0	62.8	0.22	8.59 ± 0.02	1.26 ± 0.09
C	24...40	7...11	3	1	0	11.1	0.999	8.60 ± 0.02	1.33 ± 0.04
C	24...40	7...11	1	3	0	17.1	0.99	8.58 ± 0.03	1.51 ± 0.05
D	24...50	7...11	3	1	0	33.4	0.83	8.55 ± 0.02	1.39 ± 0.05
D	24...50	7...11	1	3	0	33.7	0.82	8.54 ± 0.02	1.51 ± 0.05
E	24...50	8...9.25	3	1	0	21.8	0.86	8.55 ± 0.02	1.39 ± 0.10
E	24...50	8...9.25	1	3	0	23.7	0.78	8.55 ± 0.02	1.44 ± 0.08
f	13...50	7...11	3	3	0	97.8	0.075	8.58 ± 0.02	1.33 ± 0.04
g	13...50	8...9.25	1	3	1	44.1	0.83	8.31 ± 1.31	2.08 ± 6.09
g	13...50	8...9.25	3	1	1	37.5	0.94	8.49 ± 0.22	0.66 ± 1.08
g	13...50	8...9.25	2	3	1	38.1	0.92	8.55 ± 0.04	1.35 ± 0.06

TABLE I. Fit parameters and estimates for W_c and ν with 95% confidence intervals for the fit of $\alpha_N(W)$ for coupled planes with $\gamma = 0.9$, $m_i = 0$.

FIGURES

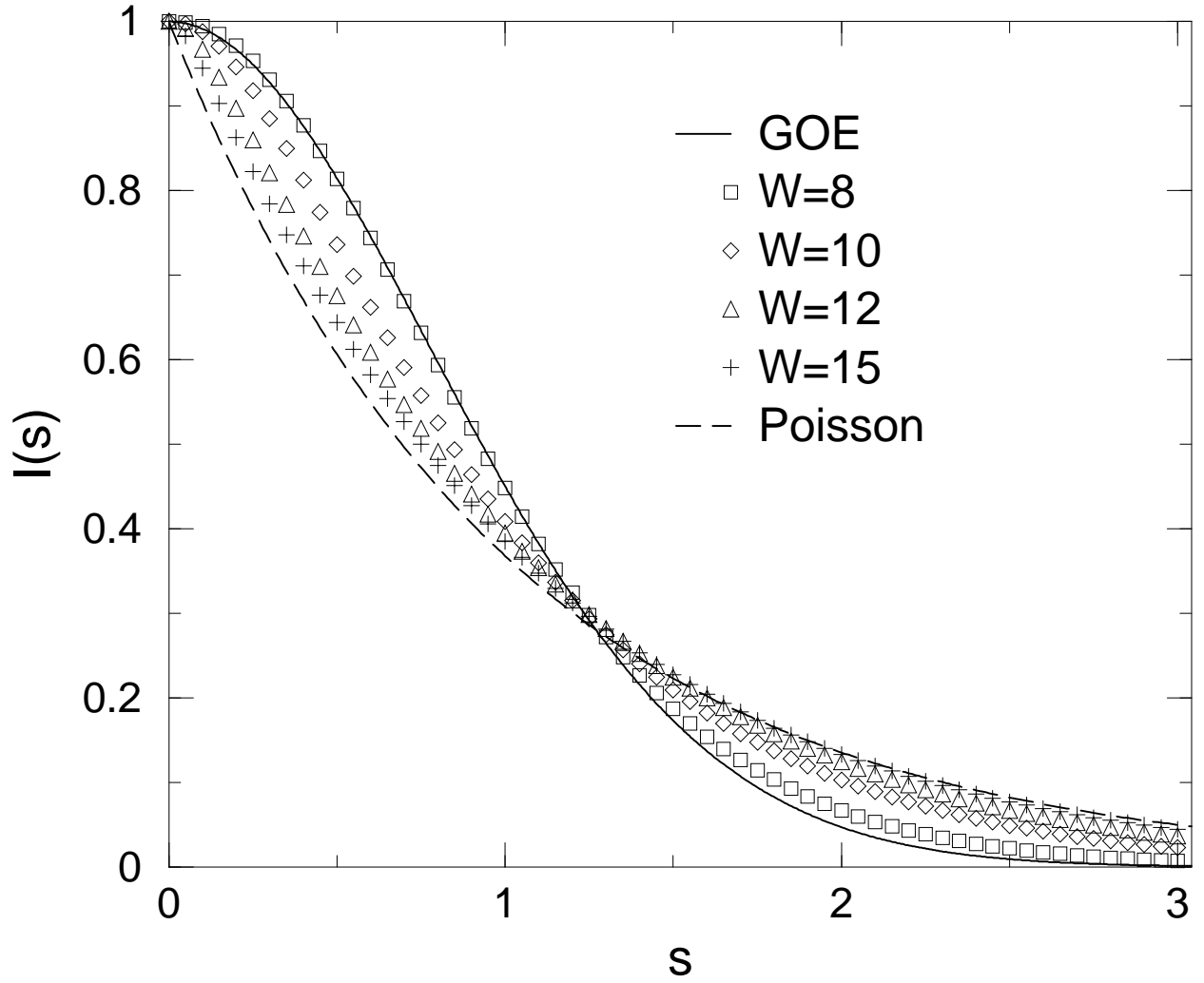


FIG. 1. Cumulative spacing distribution $I(s)$ for coupled chains with $\gamma = 0.6$ and $N = 24$ and various disorders. Solid and dashed lines indicate GOE and Poisson behavior, respectively.

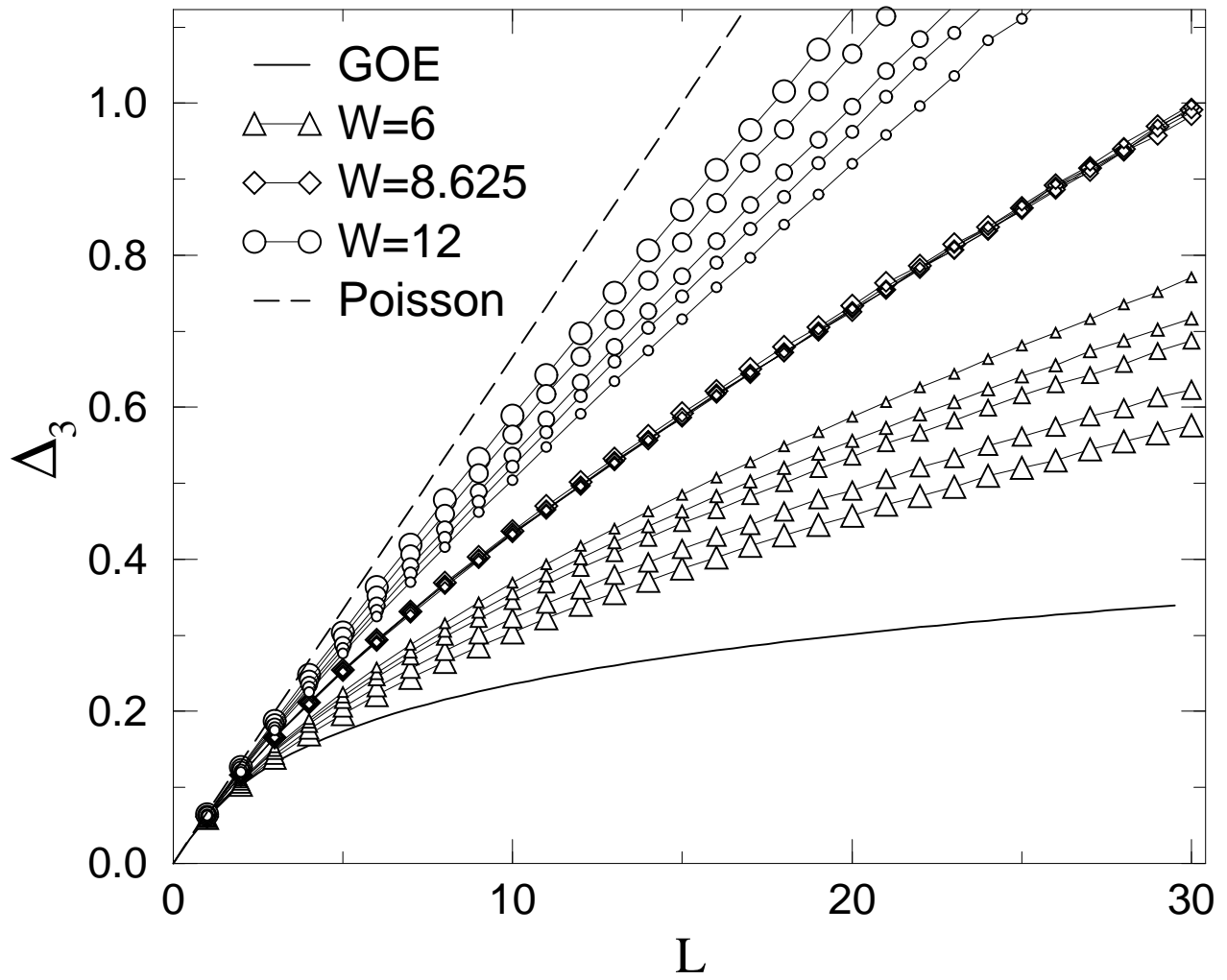


FIG. 2. Δ_3 statistics for coupled planes with $\gamma = 0.9$ and system sizes $N = 13, 17, 21, 30, 40$, indicated by increasing symbol size.

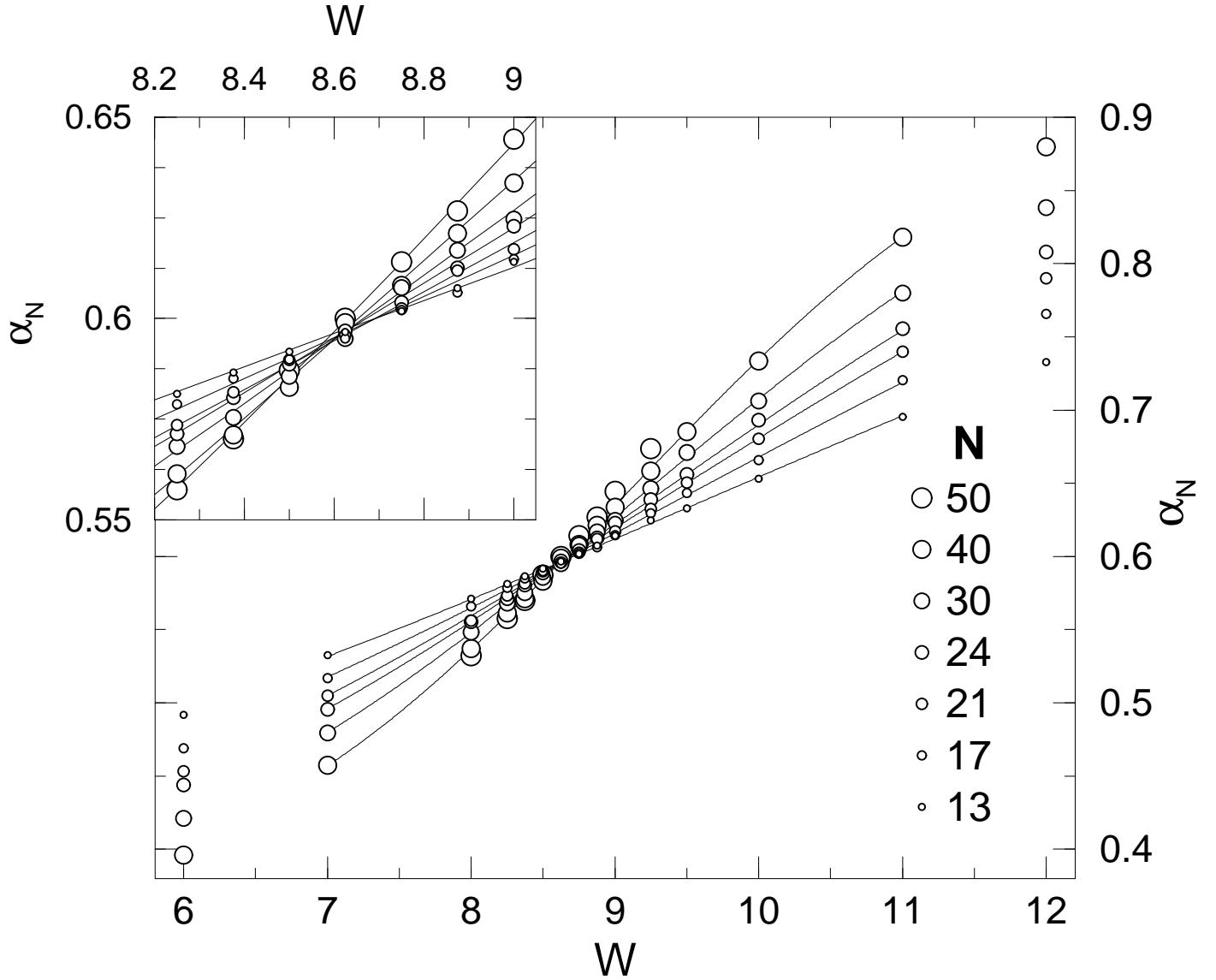


FIG. 3. The integrated Δ_3 statistics $\alpha_N(W)$ for coupled planes with $\gamma = 0.9$ as a function of disorder W for various system sizes N . The lines correspond to fit A of Table I. In the inset we show enlarged the region around the crossing point. Here, the lines are cubic fits to the data.

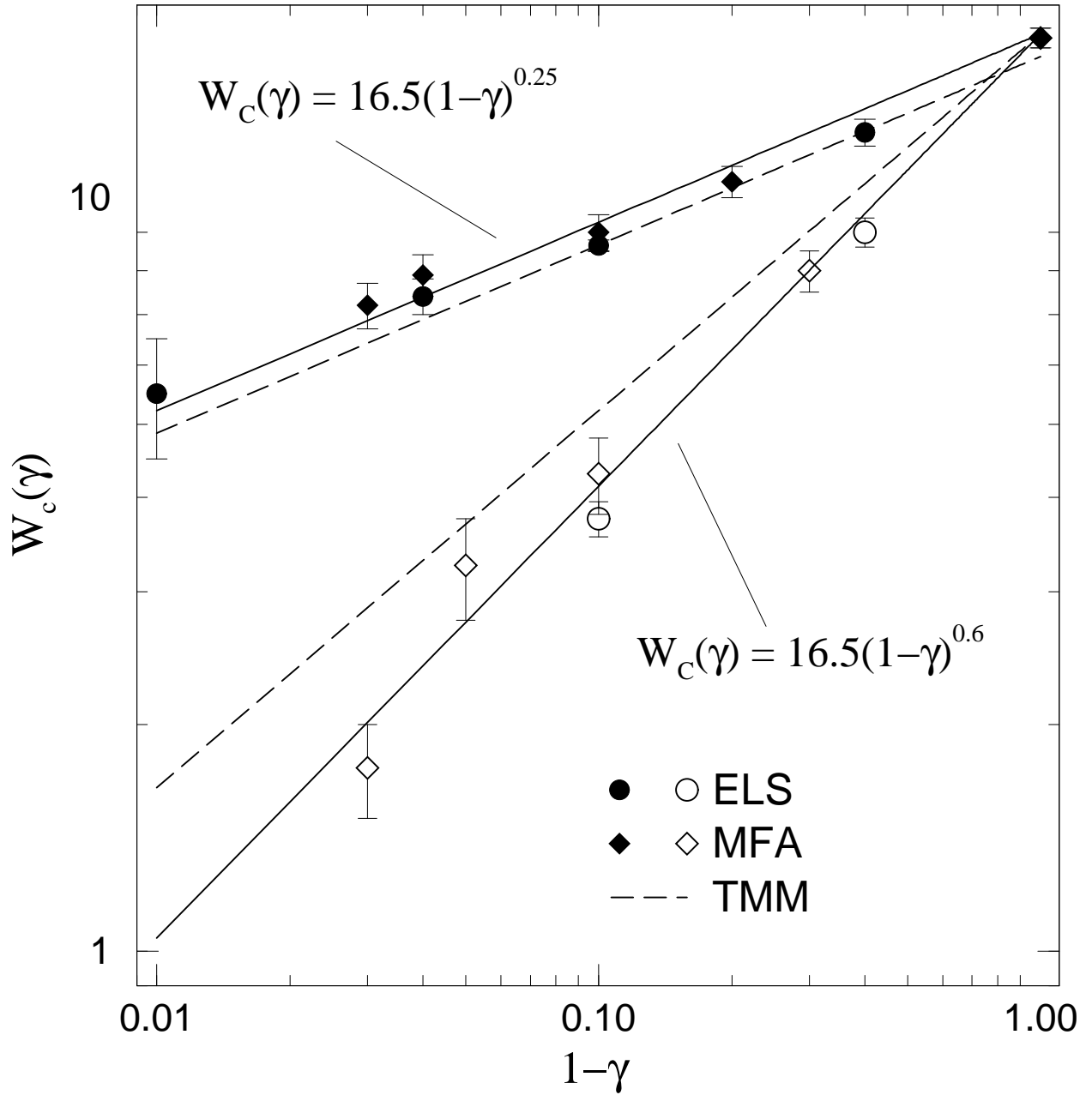


FIG. 4. Anisotropy dependence of W_c for coupled planes (filled symbols) and chains (open symbols) as computed by ELS and previously⁸ by MFA. We also added a fit to TMM data of Ref. 6 (dashed lines).

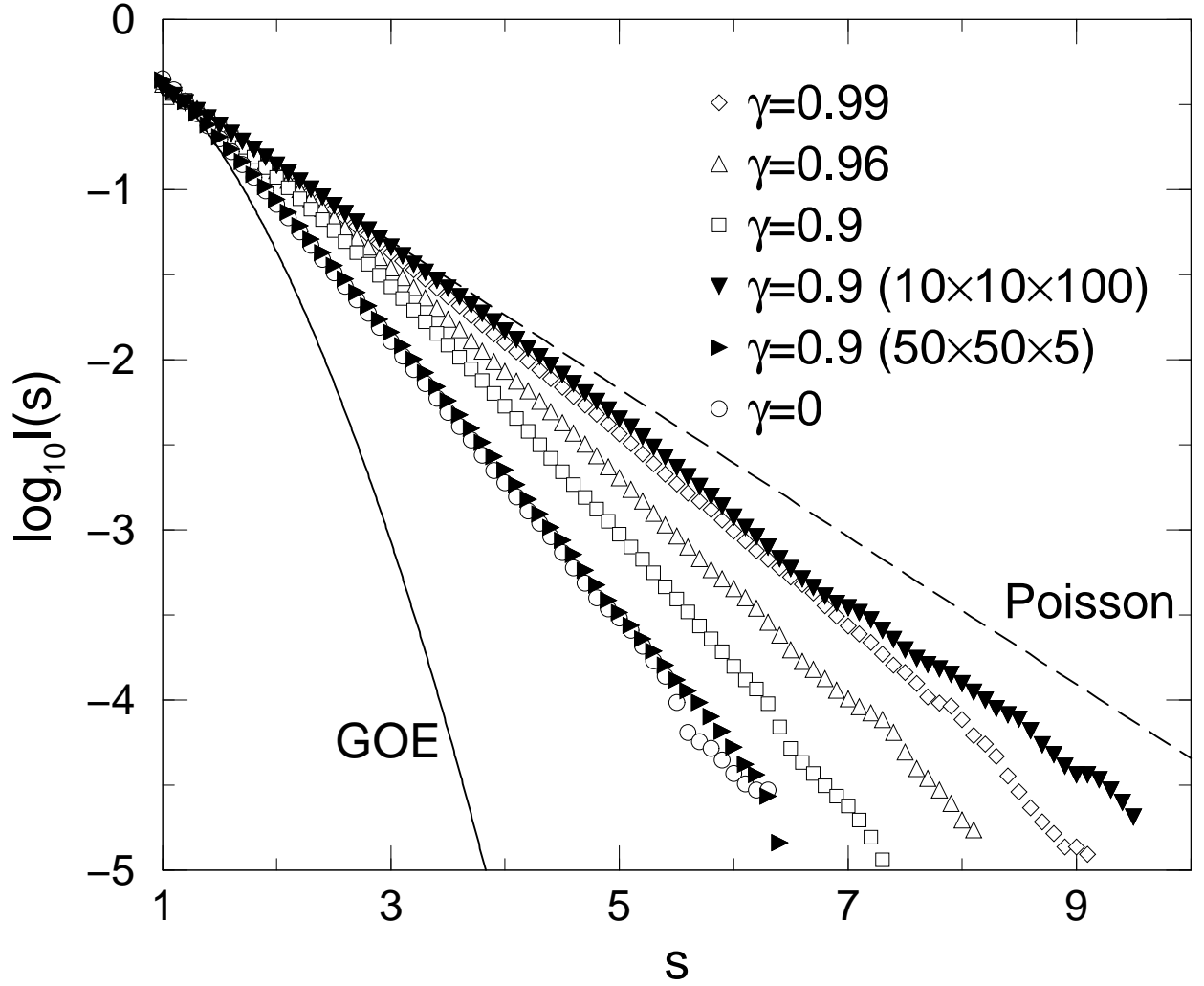


FIG. 5. Large- s behavior of the cumulative level spacing-distribution $I_c(s)$ of coupled planes at the MIT for various values of anisotropy γ . The filled symbols correspond to the non-cubic samples as discussed in Sec. III D.

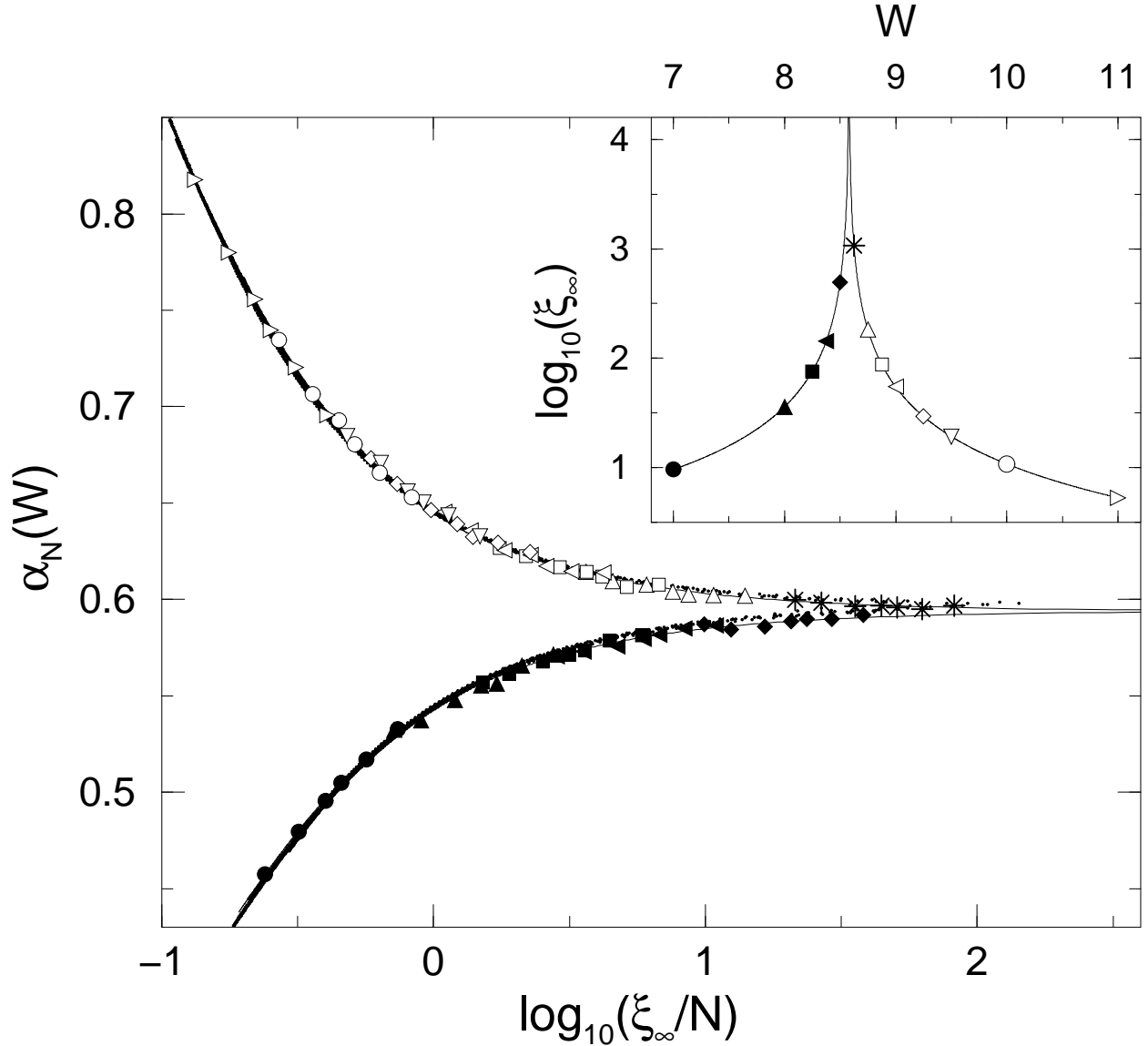


FIG. 6. Scaling function $\alpha_N = f(\xi_\infty/N)$ and scaling parameter ξ_∞ (inset) from fit f in Table I with localized (open symbols) and extended branch (filled symbols). Different symbols distinguish the data for different W . The lines are the functional forms as given by the fit. We added a scaling function (dots) obtained by a different method.¹⁷ The large number of dots partly results in a broad line.

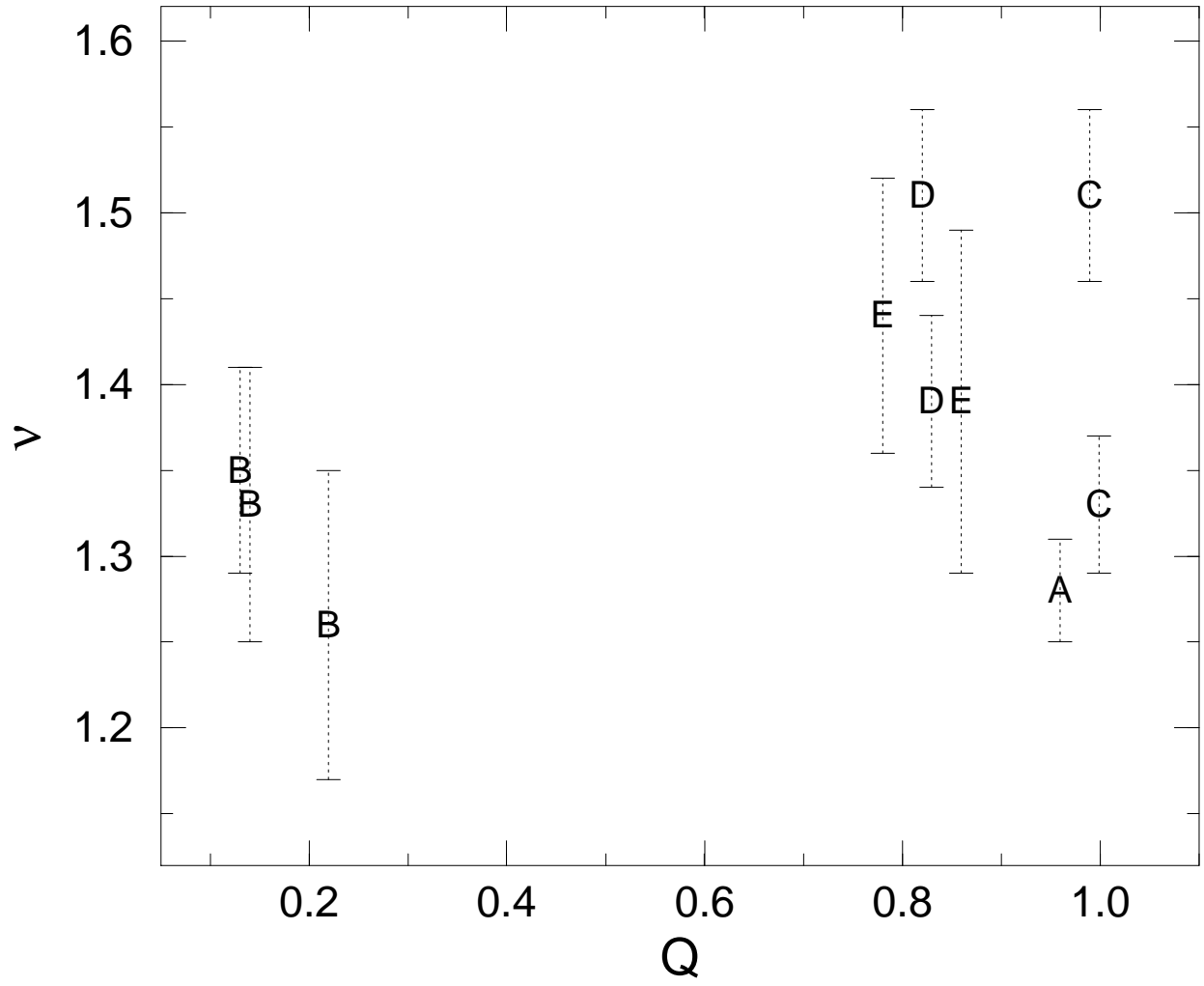


FIG. 7. Results for ν and their 95% confidence intervals for the fits of the α_N data as reported in Table I.

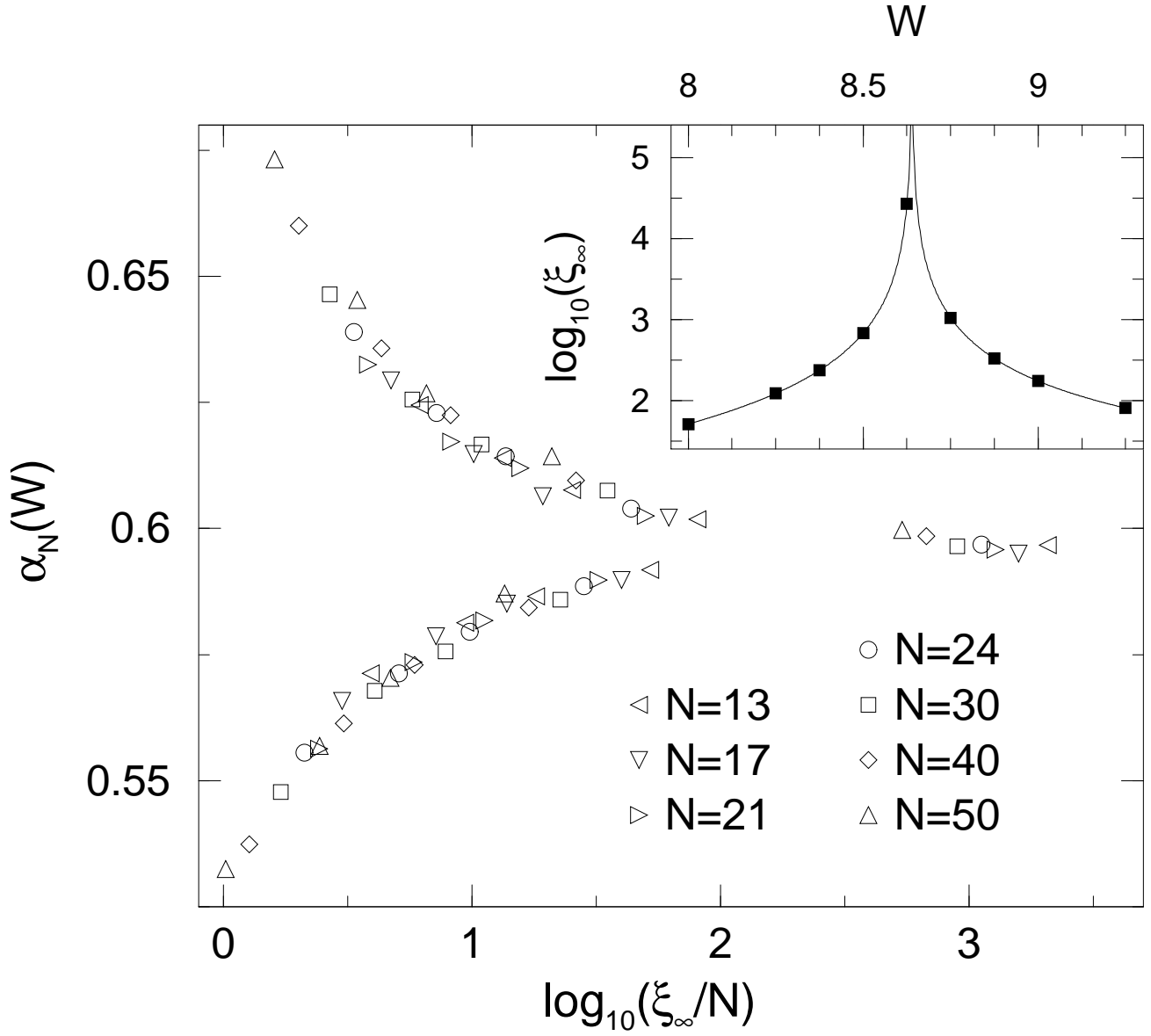


FIG. 8. $\alpha_N(W)$ for coupled planes with $\gamma = 0.9$ scaled with $\xi_\infty(W)$, as shown in the inset, taken from a fit of highly accurate TMM data with $\nu = 1.59$ of Ref. 36.